NIH Public Access
Author Manuscript
J Hepatol. Author manuscript; available in PMC 2008 April 1.

Published in final edited form as:
J Hepatol. 2008 February ; 48(2): 276–288.

Small Proline Rich Proteins (SPRR) Function as SH3 Domain Ligands, Increase Resistance to Injury and are Associated with Epithelial-Mesenchymal Transition (EMT) in cholangiocytes

Anthony J. Demetris, M.D.[1,2,*], **Susan Specht, M.S.**[1,2], **Isao Nozaki, M.D.**[1,2,+], **John G. Lunz III**[1,2,3], **Donna Beer Stolz, PhD.**[4], **Noriko Murase, M.D.**[1,3], and **Tong Wu, M.D., PhD.**[2]

1*Thomas E Starzl Transplantation Institute, University of Pittsburgh Medical Center, Pittsburgh, PA 15213*

2*Department of Pathology, Division of Transplantation, University of Pittsburgh Medical Center, Pittsburgh, PA 15213*

3*Department of Surgery, Division of Transplantation, University of Pittsburgh Medical Center, Pittsburgh, PA 15213*

4*Department of Cell Biology and Physiology, University of Pittsburgh School of Medicine, Pittsburgh, Pennsylvania 15261*

+*Isao Nozaki, M.D., National Shikoku Cancer Center Hospital, Department of Surgery, 13 Horinouchi, Matsuyama, JAPAN 790-0007*

Abstract

Background/Aims—Deficient biliary epithelial cell (BEC) expression of small proline rich protein (SPRR) 2A in IL-6-/- mice is associated with defective biliary barrier function after bile duct ligation. And numerous gene array expression studies show SPRR2A to commonly be among the most highly upregulated genes in many non-squamous, stressed and remodeling barrier epithelia. Since the function of SPRR in these circumstances is unknown, we tested the exploratory hypothesis that BEC SPRR2A expression contributes to BEC barrier function and wound repair.

Methods—The effect of SPRR2A expression was studied in primary mouse BEC cultures; in BEC cell line after forced over expression of SPRR2A; and in human livers removed at the time of liver transplantation.

Results—Forced SPRR2A over-expression showed that it functions as a SH3 domain ligand that increases resistance to oxidative injury and promotes wound restitution by enhancing migration and acquisition of mesenchymal characteristics. Low confluency non-neoplastic mouse BEC cultures show a phenotype similar to the stable transfectants, as did spindle-shaped BEC participating in atypical ductular reactions in primary biliary cirrhosis.

Conclusions—These observations suggest that SPRR2A-related BEC barrier modifications represent a novel, but widely utilized and evolutionarily conserved, response to stress that is worthy of further study.

*Address Correspondence to: A.J. Demetris, M.D., University of Pittsburgh Medical Center, UPMC Montefiore, Room E741 200 Lothrop Street, Pittsburgh, PA 15213, Phone: (412) 647-2067, Fax: (412) 647-2084, E-mail: demetrisaj@upmc.edu.

Publisher's Disclaimer: This is a PDF file of an unedited manuscript that has been accepted for publication. As a service to our customers we are providing this early version of the manuscript. The manuscript will undergo copyediting, typesetting, and review of the resulting proof before it is published in its final citable form. Please note that during the production process errors may be discovered which could affect the content, and all legal disclaimers that apply to the journal pertain.

NIH-PA Author Manuscript
NIH-PA Author Manuscript
NIH-PA Author Manuscript

NIH-PA Author Manuscript

NIH-PA Author Manuscript

NIH-PA Author Manuscript

Keywords

Cholangiocytes; Ductular Reaction; Wound Healing; Oxidative Stress; Repair; SH3 domain; EMT

INTRODUCTION

Previous studies from our laboratory show that IL-6/gp130/STAT3 signaling importantly contributes to BEC barrier function and wound healing (reviewed in (1)), as in the skin (2), and gastrointestinal tract (3). Cellular and molecular mechanisms linking enhanced IL-6/gp130/STAT3 signaling to biliary tree wound healing and barrier function include production of the cytoprotective motogen, Trefoil family factor 3 (TFF3) (4), and increased small proline rich proteins (SPRR) expression (5).

SPRR are encoded by a tandemly arranged four-member gene family (SPRR1-4) contained within a 170-kilobase region of the epidermal differentiation complex (EDC), a cluster of >50 genes located on chromosome 1q21(6) whose products are involved in epidermal differentiation. In this context, SPRR genes are regulated coordinately as part of the EDC and encode for proteins that cross-link other EDC proteins (7). SPRR1-4 are distinguished by the consensus sequence of their proline-rich central repetitive domain (7) with SPRR2 being the most diversified of all the SPRR genes (7).

The highest ratio of non-synonymous to synonymous nucleotide substitution rates on human chromosome 1 occurs between SPRR2A and SPRR2F(8) and the EDC is the most rapidly diverging gene cluster comparing human and chimpanzee genomes (9). SPRR diversity lies primarily within the regulatory regions of the SPRR2 gene family (6), which is thought to enable SPRR2 proteins to precisely modify barriers in response to diverse environmental insults (6).

In the liver, deficient SPRR2A expression in IL-$6^{-/-}$ mice after bile duct ligation is associated with a biliary barrier defect (5). In other tissues, many cDNA microarray studies show that SPRR genes ranked among those most highly upregulated during inflammation/stress, infection, and remodeling involving barrier epithelia from the lung, skin, and intestine (Table 1). SPRR2A and other SPRR family members also rank among the most highly upregulated genes in developing tissues, including the intestine, prostate, colon, and breast, where high SPRR2A expression in the developing adolescent breast bud occurs as it penetrates the mesenchyme (Table 1).

Since SPRR function(-s) in these stress-related non-squamous contexts are unknown, we tested the exploratory hypothesis that SPRR2A expression was stress and wound repair-related. First, using a biliary epithelial cell line, SG231, we studied the effect of SPRR2A over expression on wound repair and resistance to injury. Second, we studied SPRR2A mRNA and protein expression in primary cultures of non-neoplastic mouse BEC at low and high confluency to simulate “front row” epithelial cells of healing wounds and intact epithelium, respectively. “Front row” cells refers to epithelial cells closest to an open wound that lose close contacts with neighboring cells and undergo shape changes and migration needed for wound closure. Finally, we studied SPRR2A expression in diseased human liver to determine if the alterations observed, in vitro, during high SPRR expression (SG231 forced over expression and low confluency BEC) resembled BEC in diseased human livers.

NIH-PA Author Manuscript
NIH-PA Author Manuscript
NIH-PA Author Manuscript

MATERIALS AND METHODS

Cell Cultures and Establishment of Stable Transfection of SG231 Cells

Primary mouse and human BEC were cultured on collagen gels or collagen-coated plates in complete serum-free medium (C-SFM) as described (10). The human bile duct cell line, SG231 (11), was cultured as reported (10). Human SPRR2A cDNA (X53064) was generated by RT-PCR from total RNA from primary human BEC. The SPRR2A cDNA was confirmed by DNA sequencing and inserted into the GFP expressing pTracer mammalian expression vector (Invitrogen, Carlsbad, CA) creating a C-terminal His-V5-tagged SPRR2A. A pTracer plasmid without the insert was used as a control vector. SG231 cells were transfected using FuGENE 6 Transfection Reagent (Roche, Indianapolis, IN), stable transfectants selected with zeocin (1.0 mg/ml; Invitrogen), and pTracer-SPRR2A-His-V5 clones isolated by limiting dilution. Expression was confirmed by Western blot analysis.

SPRR2A expression in transfectants was knocked-down by two SPRR2A siRNAs (ID:203488; ID:42886-40nM; Ambion, Austin, TX) using lipofectamine 2000 (Invitrogen) transfection reagent. Controls were either lipofectamine only or negative control siRNA.

SYBR Green Quantitative Real-time RT-PCR

Gene expression was quantified by SYBR Green real-time RT-PCR using primers described in Table 2. Gene expression was normalized to mouse GAPDH or human β-actin expression.

Migration Assay

Using a modified protocol for fibroblasts (12), a linear wound was created with a rubber policeman in confluent BEC monolayers. Images taken at 0h and 24h after wounding were compared and the distance traveled by the cells at the acellular front was measured. Additionally, the number of cells migrating through the pores (8μm) of a transwell (Corning, Lowell, MA) in 24 hours was measured.

Western Blot Analysis

Protein was extracted using Chaps or RIPA buffer with protease inhibitors and Western blotting performed as described (13) (Table 3). Signals were detected using enhanced chemiluminescence reagents (NEN; Life Science Products, Boston, MA) and quantified using Image J software.

Immunoprecipitation Studies

Stable SPRR2A and vector control transfectants were subjected to protein cross-linking using 2mM disuccinimidyl suberate (Pierce Biotechnology, Inc. Rockford, IL) according to the manufacturer's protocol. Protein was extracted with non-denaturing lysis buffer (1% Triton X-100, 50mM Tris(pH 7.4), 300mM NaCl, 5mM EDTA) containing protease inhibitors. 1mg of protein was immunoprecipitated with 3μg of anti-V5 or anti-C-Src(H-12) antibody (Table 2) at 4°C for 1 hour followed by rotation with 50μl of protein G agarose beads (Santa Cruz Biotechnology) at 4°C overnight. Bead-bound proteins were released by heating to 98°C in gel loading buffer and separated by SDS-PAGE.

Immunohistochemistry

Immunofluorescence and immunoperoxidase staining (Table 3) was performed as described (5).

NIH-PA Author Manuscript

NIH-PA Author Manuscript

NIH-PA Author Manuscript

Flow cytometry

Cell viability after H_2O_2 exposure was assessed by staining with propidium iodide and flow cytometric analysis on a Coulter EPICS-XL.

TRAP Assay

Total Radical Trapping Antioxidant Potential (TRAP) was determined by a luminometric method (14,15). The azo compound 2,2'-azo-bis-(2-methyl-propanimidamide)(AAPH; Cayman Chemical, Ann Arbor, MI) undergoes a constant rate of peroxidation, generating free radicals detected by luminol fluorescence. Absorption of AAPH generated radicals is first measured using a known anti-oxidant (Trolox®) as an internal standard. The induction time measures the time that Trolox® prevents the presence of free radicals and fluorescence of luminol. Extension of the Trolox® induction time by cellular lysates reflects their cellular anti-oxidant potential. SPRR2A transfected SG231 cells were lysed in water, sonicated on ice and supernatants collected after centrifugation (10,00xg; 5 minutes). Assay Reaction: 200μl luminol (PerkinElmer, Wellesley, MA), 5μg protein lysate, 10mM AAPH, 100nM Trolox®. The blank contained water instead of cytosol. Graphs (counts per second versus time) were used to determine induction times by extrapolating to 0 CPS using the maximum slope of Trolox® consumption.

Statistical Analysis

Values shown for various tests are the mean ± SD (or SE where noted) with experimental repeats of $n \geq 3$. A student's t-test with $\alpha = 0.05$ was used to compare two groups.

RESULTS

Association of SPRR2A Expression with Changes in Cell Shape

SPRR2A was stably transfected into the BEC line, SG231. This line was chosen because it was derived from, and maintains, most characteristics of mature intrahepatic BEC, including a distinctly epithelial morphology with clear apical/basal polarization, mucin production, surface micro-villi, and BEC phenotypic markers (11). It also shows responses to cytokines and growth factors similar to mature BEC (16). Stable SPRR2A clones showed 10 to 17 times the level of SPRR2A mRNA/protein expression than normal human BEC (Figure 1). This compares favorably with the ≥ 14-fold increase seen in BEC after bile duct ligation, but significantly less than increases seen in intestinal epithelial cells following surgical or infectious stressors (Table 1).

Compared to control transfectants, all SPRR2A stable transfectants showed features of front row cells, such as cell enlargement, extension of cytoplasmic processes, and partial disruption of contact with neighboring cells (Figure 1C). Consistent with at least partial EMT occurring in front row cells, E-cadherin and CK-19 protein expression was uniformly decreased in all SPRR2A clones (Figure 1D). Clones (1, 3, and 5) that maintained some epithelioid morphology still showed disruption of close contacts with neighboring cells and significantly decreased E-cadherin and CK19 expression. Dendritic-shaped clones tended to lose E-cadherin and CK19 expression altogether and acquired mesenchymal characteristics. Clone 7, which showed intermediate changes, was chosen for further analysis.

Immunofluorescence staining of control transfectants for E-cadherin, connexin-43, cytokeratin-19, vimentin, F-actin and fibronectin (17) showed an expression pattern typical of epithelial cells (Figure 2A). Clone 7, in contrast, lost many epithelial and gained several mesenchymal cell characteristics (Figure 2A). SPRR2A specific siRNA treatment reversed these effects in clone 7, significantly increasing CK19 expression and improving epithelial sheet morphology (Figure 2B).

NIH-PA Author Manuscript

NIH-PA Author Manuscript

NIH-PA Author Manuscript

Non-confluent BEC cultures also assume a front row, large spreading, phenotype until they reach confluence when a typical cobblestone monolayer is formed. We predicted, therefore, that SPRR2A expression would be increased in non-confluent BEC cultures and decrease upon confluence. Consistent with expectations, SPRR2A expression was 5-fold higher in widely scattered non-confluent BEC cultures and *decreased* significantly as BEC monolayers reached confluence (Figure 3A). Vimentin and S100A4 mRNA expression were increased at low confluency and decreased with confluence, whereas E-cadherin mRNA expression increased with confluence, except at the final phase when a dense typical cobblestone sheet had already formed. CK19 expression remained relatively stable throughout.

We next tested whether confluence affected E-cadherin and CK-19 levels in the SPRR2A transfectants and the vector control. E-cadherin and CK-19 levels increased at high confluence, but expression levels in the SPRR2A transfectants always remained significantly less than controls (Figure 3B). Clone 7 never formed typical compact cobblestone sheets, regardless of the level of confluence. Thus, forced SPRR2A expression in SG231 cells appears to maintain them in a “front row” phenotype, overcoming the tendency to form intact epithelial sheets seen in the vector controls.

The Effect of SPRR2A Expression on Cell Migration

Since SPRR2A transfectants mimic “front row” epithelial cells of wounds (18), we tested their ability to effect wound closure in a migration assay, in vitro (4). Despite decreased proliferation (Figure 4A), SPRR2A transfectants showed significantly better restitution/migration that was not affected by preventing proliferation with hydroxyurea (Figure 4B). Inhibition of SPRR2A expression using SPRR2A specific siRNA (Figure 4C) reversed the enhanced migration (Figure 4D). The SPRR2A-expressing clones also had an increased ability to transverse through the pores of a transwell (Figure 4E).

Analysis of Potential SPRR2A Binding Partners

SPRR2A serves as a cross-linking protein during formation of the cornified envelope, but other EDC constituents are not equally upregulated during non-coordinate SPRR2A expression in non-squamous tissues, including BEC (5). This suggests that SPRR2A has other binding partners and functions under these circumstances. Examination of the SPRR2A proline rich sequence revealed putative SH3 domain ligand motifs (Figure 5A).

Speculation about potential binding partners included the SH3 homology domain (Figure 5A) of Src family kinases (SFK) because they critically influence epithelial cell-to-cell junction formation (19). A SH3 domain array analysis confirmed SPPR2A binding to several SH3 domain-containing proteins (Figure 5B). Two of these proteins are SFK (Yes1 and c-Src) (20), which are intimately involved in cell junction formation, as is abl (21), another strong binding partner. Immunoprecipitation studies from SPRR2A transfectants confirmed that SPRR2A-Src (Figure 5C) and SPRR2A-Yes (data not shown) complexes formed spontaneously, in vivo. Finally, immunofluorescence studies showed that the intra-cellular localization of the SPRR2A binding partner, Src, changed after SPRR2A transfection (Figure 5D).

SPRR2A Protects Cells from Injury

BEC participating in ductular reactions, or wound repair, enjoy a survival advantage over hepatocytes and are more resistant than hepatocytes to oxidative stress (22). Since STAT3-dependent BEC SPRR2A expression is seen during stress and remodeling (5) they should also be more resistant to injury.

NIH-PA Author Manuscript

NIH-PA Author Manuscript

NIH-PA Author Manuscript

Cell death after H_2O_2-induced injury was monitored by propidium iodide staining (Figure 6A) and the release of HMGB1 (Figure 6B) and showed that SPRR2A transfectants were more resistant than vector-transfected controls. SPRR2-associated resistance to injury was reversible by siRNA inhibition of SPRR2A expression (Figure 6B). The SPRR2A transfectants were also more resistant to glycochenodeoxycholate (GCDC)-induced injury (Figure 6C), which is directly relevant to wound healing conditions in the biliary tree.

Amino acids, peptides, and proteins have relatively low specific anti-oxidant activity, on a molar basis, but represent an important scavenger of ROS because of relatively high intracellular molar concentrations. The overall cytosolic reducing power can be measured in the Total Radical Trapping Anti-oxidant Potential (TRAP) assay, measuring the time cytosolic extracts can quench the oxidizing potential of AAPH (See Methods). Compared to vector controls the SPRR2A transfectants significantly delayed maximum oxygen uptake by the probe, consistent with a greater reducing power (Figure 6D).

Expression of SPRR2A mRNA and Protein in Diseased Human Livers

We next measured SPRR2A mRNA expression by real-time PCR in normal and in diseased human liver tissue. Figure 7A-B shows that more IL-6 and SPRR2A mRNA are expressed in primary biliary cirrhosis (PBC) than in normal livers. The apparent discrepancy between IL-6 and SPRR2A expression in alcoholic liver disease is likely related to inhibition of STAT3 activity seen in that disorder (23).

In diseased livers SPRR2 protein localized to BEC (Figure 7C-E), consistent with previous results (5). In PBC, SPRR2 localized to the cytoplasmic periphery in damaged columnar-shaped BEC lining septal bile ducts, which co-expressed SPRR2 and cytokeratin but not vimentin (Figure 7D). Diffuse cytoplasmic SPRR2 localization occurred in some spindle-shaped BEC participating in “atypical” ductular reactions (24), characterized by an anastomosing network of ductules, with poorly defined lumina, lined by flattened cells with scant cytoplasm (24) (Figure 7E). Atypical ductules are encountered most commonly in chronic cholestatic diseases, especially PBC (28). Some atypical spindle-shaped BEC were also focally vimentin and cytokeratin positive (Figure 7E), indicative of a phenotype intermediate between epithelial and mesenchymal cells and similar to the SPRR2A transfectants and low-confluency mouse BEC cultures, in vitro. Immunofluorescence staining of PBC, PSC, and chronic hepatitis livers showed that BEC SPRR2 expression was strongest and most prevalent in PBC, especially in damaged small septal bile ducts and in atypical ductular reactions.

DISCUSSION

In wounded barrier epithelia, front row cells often undergo partial or complete dissolution of cell-cell contacts and acquire some mesenchymal characteristics. This functions to disaggregate epithelial units and reshape epithelia for movement (17). Epithelia in transition lose polarity, intercellular junctions, and down-regulate cytokeratin filaments in order to rearrange F-actin stress fibers and express filopodia and lamellopodia (17). Several lines of evidence show that SPRR2 expression is associated with this process.

Forced non-coordinate expression of SPRR2A in SG231 cells, in vitro, can lead to a front row phenotype. Since SG231 is a cell line the results should be interpreted with some caution. But non-neoplastic BEC with similar phenotypic characteristics were also observed in low-confluency primary mouse BEC cultures and in atypical ductules in PBC. SPRR2A is also expressed exclusively in the remodeling biliary tree after bile duct ligation (5), and in many injured and remodeling barrier epithelia from the lung, skin, uterus, and intestine after exposure to injury and stress (Table 1). It seems reasonable, therefore, to suggest that SPRR2A upregulation is a stress-related response that helps to protect barrier epithelium from oxidative

NIH-PA Author Manuscript

NIH-PA Author Manuscript

NIH-PA Author Manuscript

damage and prepares it for remodeling. It would have been ideal to conditionally block biliary SPRR expression to further investigate SPRR function. But this approach has not been feasible because of redundancy and regulatory diversity in the SPRR gene locus.

Molecular studies show that non-coordinate BEC expression makes SPRR2A available for binding to SH3 domain-containing proteins (25), such as c-Src, c-Yes, and abl. Other binding partners exist. These particular molecules, however, contribute significantly to formation and maintenance of intercellular junctions, shape changes (20,26), and to acquisition of some mesenchymal characteristics (19,27).

As seen in the protein binding array, promiscuity of SH3 ligand binding enables numerous potential interactions and facilitates assembly of large multi-molecular complexes. This can lead to context specific effects (28). It is likely, therefore, that SPRR expression might not always produce the same effects, but be dependent on the cell proteome at the time of SPRR expression. This likely accounts for some of the variability seen in our different SPRR2A clones and that Sprr2 is expressed in damaged septal bile ducts and in atypical cholangioles, which differ in their vimentin expression.

Spindle-shaped atypical ductules in PBC can acquire some mesenchymal characteristics similar to the SPRR2A transfectants and low confluency mouse BEC. In embryonic liver ductal plate BEC transiently express vimentin (29) and down-regulate membranous E-cadherin (30) when they “invade” the portal connective tissue to form mature intrahepatic bile ducts. SPRR2A is also highly upregulated when mouse hepatoblasts transform into BEC after exposure to Matrigel (http://www.ncbi.nlm.nih.gov/projects/geo/gds/gds_browse.cgi?gds=970). During injury and repair (1), BEC can transform from polarized cuboidal epithelial cells into spindle-shaped migratory cells that can express vimentin (31). However, since BEC appear to retain some epithelial characteristics during this process, BEC EMT may not be exactly the same as described for kidney tubular epithelial cells (17). Instead, acquisition of mesenchymal characteristics in BEC may be “meta-stable” because they appear to revert to an epithelial phenotype when migration/repair is complete. More study is needed on this topic.

Among liver diseases tested, SPRR2A is most highly expressed in BEC of small atypical ductules from PBC livers, and to a lesser extent in other diseases. It was clear, however, that EMT changes were more common in atypical ductular reactions. It is likely, therefore, that the heterogeneity of BEC in large versus small ducts (32) accounts for this difference. In the uterus, however, SPRR2A is highly upregulated in an estrogen-dependent fashion at the blastocyst implantation site where decreased intercellular junctions, desmoplakin, and cytokeratin are also seen (33). The possibility that estrogen and IL-6 co-dependent BEC barrier modifications might be involved in PBC pathogenesis is also worthy of further study.

This study focuses specifically on BEC but the ubiquity and magnitude of non-coordinate SPRR expression in non-squamous tissues, suggests that it is part of a generic stress/remodeling response. Although not described in mammalian cells, proline utilization is widely recognized as an anti-stress response in plants (34). Proline residues in proline-rich proteins can be converted to either 4- or 5-hydroxy proline by ROS and these changes will not cause cleavage of the polypeptide or damage the amino acid backbone (34).

In conclusion, our studies suggest that SPRR upregulation is a widely utilized stress and remodeling response which contributes to barrier function, wound repair and increase resistance to injury. This may explain why the gene locus is so rapidly diverging (9) and a “hot-spot” for non-synonymous substitutions (8).

NIH-PA Author Manuscript

NIH-PA Author Manuscript

NIH-PA Author Manuscript

Acknowledgements

Supported by National Institutes of Health grant DK49615 (A.J.D.), CA76541 (D.B.S.), and CA 102325 (T.W.).

References

1. Demetris AJ, Fontes P, Lunz JG 3rd, Specht S, Murase N, Marcos A. Wound healing in the biliary tree of liver allografts. Cell Transplant 2006;15(Suppl 1):S57–65. [PubMed: 16826796]
2. Lin ZQ, Kondo T, Ishida Y, Takayasu T, Mukaida N. Essential involvement of IL-6 in the skin wound-healing process as evidenced by delayed wound healing in IL-6-deficient mice. J Leukoc Biol 2003;73:713–721. [PubMed: 12773503]
3. Tebbutt NC, Giraud AS, Inglese M, Jenkins B, Waring P, Clay FJ, et al. Reciprocal regulation of gastrointestinal homeostasis by SHP2 and STAT-mediated trefoil gene activation in gp130 mutant mice. Nat Med 2002;8:1089–1097. [PubMed: 12219085]
4. Nozaki I, Lunz JG 3rd, Specht S, Park JI, Giraud AS, Murase N, et al. Regulation and function of trefoil factor family 3 expression in the biliary tree. Am J Pathol 2004;165:1907–1920. [PubMed: 15579435]
5. Nozaki I, Lunz JG 3rd, Specht S, Stolz DB, Taguchi K, Subbotin VM, et al. Small proline-rich proteins 2 are noncoordinately upregulated by IL-6/STAT3 signaling after bile duct ligation. Lab Invest 2005;85:109–123. [PubMed: 15558059]
6. Cabral A, Voskamp P, Cleton-Jansen AM, South A, Nizetic D, Backendorf C. Structural organization and regulation of the small proline-rich family of cornified envelope precursors suggest a role in adaptive barrier function. J Biol Chem 2001;276:19231–19237. [PubMed: 11279051]
7. Patel S, Kartasova T, Segre JA. Mouse Sprr locus: a tandem array of coordinately regulated genes. Mamm Genome 2003;14:140–148. [PubMed: 12584609]
8. Gregory SG, Barlow KF, McLay KE, Kaul R, Swarbreck D, Dunham A, et al. The DNA sequence and biological annotation of human chromosome 1. Nature 2006;441:315–321. [PubMed: 16710414]
9. Initial sequence of the chimpanzee genome and comparison with the human genome. Nature 2005;437:69–87. [PubMed: 16136131]
10. Yokomuro S, Lunz JG, Sakamoto T, Ezure T, Murase N, Demetris AJ. The effect of interleukin-6 (IL-6)/gp130 signalling on biliary epithelial cell growth, in vitro. Cytokine 2000;12:727–730. [PubMed: 10843753]
11. Storto PD, Saidman SL, Demetris AJ, Letessier E, Whiteside TL, Gollin SM. Chromosomal breakpoints in cholangiocarcinoma cell lines. Genes Chromosomes Cancer 1990;2:300–310. [PubMed: 2176543]
12. Chen P, Gupta K, Wells A. Cell movement elicited by epidermal growth factor receptor requires kinase and autophosphorylation but is separable from mitogenesis. J Cell Biol 1994;124:547–555. [PubMed: 8106552]
13. Ni R, Nishikawa Y, Carr BI. Cell growth inhibition by a novel vitamin K is associated with induction of protein tyrosine phosphorylation. J Biol Chem 1998;273:9906–9911. [PubMed: 9545333]
14. Valkonen M, Kuusi T. Spectrophotometric assay for total peroxyl radical-trapping antioxidant potential in human serum. J Lipid Res 1997;38:823–833. [PubMed: 9144097]
15. Krasowska A, Rosiak D, Szkapiak K, Lukaszewicz M. Chemiluminescence detection of peroxyl radicals and comparison of antioxidant activity of phenolic compounds. Current Topics in Biophysics 2000;92:89–95.
16. Yokomuro S, Tsuji H, Lunz JG 3rd, Sakamoto T, Ezure T, Murase N, et al. Growth control of human biliary epithelial cells by interleukin 6, hepatocyte growth factor, transforming growth factor beta1, and activin A: comparison of a cholangiocarcinoma cell line with primary cultures of non-neoplastic biliary epithelial cells. Hepatology 2000;32:26–35. [PubMed: 10869285]
17. Kalluri R, Neilson EG. Epithelial-mesenchymal transition and its implications for fibrosis. J Clin Invest 2003;112:1776–1784. [PubMed: 14679171]
18. Yamada T, Aoyama Y, Owada MK, Kawakatsu H, Kitajima Y. Scraped-wounding causes activation and association of C-Src tyrosine kinase with microtubules in cultured keratinocytes. Cell Struct Funct 2000;25:351–359. [PubMed: 11280705]

NIH-PA Author Manuscript NIH-PA Author Manuscript NIH-PA Author Manuscript

19. Avizienyte E, Fincham VJ, Brunton VG, Frame MC. Src SH3/2 domain-mediated peripheral accumulation of Src and phospho-myosin is linked to deregulation of E-cadherin and the epithelial-mesenchymal transition. Mol Biol Cell 2004;15:2794–2803. [PubMed: 15075377]
20. Frame MC. Src in cancer: deregulation and consequences for cell behaviour. Biochim Biophys Acta 2002;1602:114–130. [PubMed: 12020799]
21. Lilien J, Balsamo J. The regulation of cadherin-mediated adhesion by tyrosine phosphorylation/dephosphorylation of beta-catenin. Curr Opin Cell Biol 2005;17:459–465. [PubMed: 16099633]
22. Lunz JG 3rd, Tsuji H, Nozaki I, Murase N, Demetris AJ. An inhibitor of cyclin-dependent kinase, stress-induced p21Waf-1/Cip-1, mediates hepatocyte mito-inhibition during the evolution of cirrhosis. Hepatology 2005;41:1262–1271. [PubMed: 15880761]
23. Chen J, Kunos G, Gao B. Ethanol rapidly inhibits IL-6-activated STAT3 and C/EBP mRNA expression in freshly isolated rat hepatocytes. FEBS Lett 1999;457:162–168. [PubMed: 10486586]
24. Fabris L, Strazzabosco M, Crosby HA, Ballardini G, Hubscher SG, Kelly DA, et al. Characterization and isolation of ductular cells coexpressing neural cell adhesion molecule and Bcl-2 from primary cholangiopathies and ductal plate malformations. Am J Pathol 2000;156:1599–1612. [PubMed: 10793072]
25. Kay BK, Williamson MP, Sudol M. The importance of being proline: the interaction of proline-rich motifs in signaling proteins with their cognate domains. Faseb J 2000;14:231–241. [PubMed: 10657980]
26. Clump DA, Qazi IH, Sudol M, Flynn DC. c-Yes response to growth factor activation. Growth Factors 2005;23:263–272. [PubMed: 16338789]
27. Summy JM, Sudol M, Eck MJ, Monteiro AN, Gatesman A, Flynn DC. Specificity in signaling by c-Yes. Front Biosci 2003;8:s185–205. [PubMed: 12456296]
28. Mayer BJ. SH3 domains: complexity in moderation. J Cell Sci 2001;114:1253–1263. [PubMed: 11256992]
29. Haruna Y, Saito K, Spaulding S, Nalesnik MA, Gerber MA. Identification of bipotential progenitor cells in human liver development. Hepatology 1996;23:476–481. [PubMed: 8617427]
30. Terada T, Ashida K, Kitamura Y, Matsunaga Y, Takashima K, Kato M, et al. Expression of epithelial-cadherin, alpha-catenin and beta-catenin during human intrahepatic bile duct development: a possible role in bile duct morphogenesis. J Hepatol 1998;28:263–269. [PubMed: 9514539]
31. Nakanuma Y, Kono N. Expression of vimentin in proliferating and damaged bile ductules and interlobular bile ducts in nonneoplastic hepatobiliary diseases. Modern Pathology 1992;5:550–554. [PubMed: 1285354]
32. Kanno N, LeSage G, Glaser S, Alvaro D, Alpini G. Functional heterogeneity of the intrahepatic biliary epithelium. Hepatology 2000;31:555–561. [PubMed: 10706542]
33. Illingworth IM, Kiszka I, Bagley S, Ireland GW, Garrod DR, Kimber SJ. Desmosomes are reduced in the mouse uterine luminal epithelium during the preimplantation period of pregnancy: a mechanism for facilitation of implantation. Biol Reprod 2000;63:1764–1773. [PubMed: 11090447]
34. Matysik J, Alia, Bhalu B, Mohanty P. Molecular mechanisms of quenching of reactive oxygen species by proline under stress in plants. Current Science 2002;82:525–532.
35. Hooper LV, Wong MH, Thelin A, Hansson L, Falk PG, Gordon JI. Molecular analysis of commensal host-microbial relationships in the intestine. Science 2001;291:881–884. [PubMed: 11157169]
36. Knight PA, Pemberton AD, Robertson KA, Roy DJ, Wright SH, Miller HR. Expression profiling reveals novel innate and inflammatory responses in the jejunal epithelial compartment during infection with Trichinella spiralis. Infect Immun 2004;72:6076–6086. [PubMed: 15385512]
37. Abgueguen E, Toutain B, Bedrine H, Chicault C, Orhant M, Aubry M, et al. Differential expression of genes related to HFE and iron status in mouse duodenal epithelium. Mamm Genome 2006;17:430–450. [PubMed: 16688533]
38. Mueller A, O'Rourke J, Grimm J, Guillemin K, Dixon MF, Lee A, et al. Distinct gene expression profiles characterize the histopathological stages of disease in Helicobacter-induced mucosa-associated lymphoid tissue lymphoma. Proc Natl Acad Sci U S A 2003;100:1292–1297. [PubMed: 12552104]
39. Stern LE, Erwin CR, Falcone RA, Huang FS, Kemp CJ, Williams JL, et al. cDNA microarray analysis of adapting bowel after intestinal resection. J Pediatr Surg 2001;36:190–195. [PubMed: 11150463]

NIH-PA Author Manuscript

NIH-PA Author Manuscript

NIH-PA Author Manuscript

40. Sun FJ, Kaur S, Ziemer D, Banerjee S, Samuelson LC, De Lisle RC. Decreased gastric bacterial killing and up-regulation of protective genes in small intestine in gastrin-deficient mouse. Dig Dis Sci 2003;48:976–985. [PubMed: 12772799]
41. Tan YF, Li FX, Piao YS, Sun XY, Wang YL. Global gene profiling analysis of mouse uterus during the oestrous cycle. Reproduction 2003;126:171–182. [PubMed: 12887274]
42. Hong SH, Nah HY, Lee JY, Lee YJ, Lee JW, Gye MC, et al. Estrogen regulates the expression of the small proline-rich 2 gene family in the mouse uterus. Mol Cells 2004;17:477–484. [PubMed: 15232223]
43. Zimmermann N, Doepker MP, Witte DP, Stringer KF, Fulkerson PC, Pope SM, et al. Expression and regulation of small proline-rich protein 2 in allergic inflammation. Am J Respir Cell Mol Biol 2005;32:428–435. [PubMed: 15731505]
44. Vos JB, Datson NA, van Kampen AH, Luyf AC, Verhoosel RM, Zeeuwen PL, et al. A molecular signature of epithelial host defense: comparative gene expression analysis of cultured bronchial epithelial cells and keratinocytes. BMC Genomics 2006;7:9. [PubMed: 16420688]
45. Domachowske JB, Bonville CA, Easton AJ, Rosenberg HF. Differential expression of proinflammatory cytokine genes in vivo in response to pathogenic and nonpathogenic pneumovirus infections. J Infect Dis 2002;186:8–14. [PubMed: 12089656]
46. Sandler NG, Mentink-Kane MM, Cheever AW, Wynn TA. Global gene expression profiles during acute pathogen-induced pulmonary inflammation reveal divergent roles for Th1 and Th2 responses in tissue repair. J Immunol 2003;171:3655–3667. [PubMed: 14500663]
47. Yoneda K, Chang MM, Chmiel K, Chen Y, Wu R. Application of high-density DNA microarray to study smoke- and hydrogen peroxide-induced injury and repair in human bronchial epithelial cells. J Am Soc Nephrol 2003;14:S284–289. [PubMed: 12874447]
48. Kawasaki S, Kawamoto S, Yokoi N, Connon C, Minesaki Y, Kinoshita S, et al. Up-regulated gene expression in the conjunctival epithelium of patients with Sjogren's syndrome. Exp Eye Res 2003;77:17–26. [PubMed: 12823984]
49. Young PP, Modur V, Teleron AA, Ladenson JH. Enrichment of genes in the aortic intima that are associated with stratified epithelium: implications of underlying biomechanical and barrier properties of the arterial intima. Circulation 2005;111:2382–2390. [PubMed: 15867175]
50. Pradervand S, Yasukawa H, Muller OG, Kjekshus H, Nakamura T, St Amand TR, et al. Small proline-rich protein 1A is a gp130 pathway- and stress-inducible cardioprotective protein. Embo J 2004;23:4517–4525. [PubMed: 15510217]
51. Gotter J, Brors B, Hergenhahn M, Kyewski B. Medullary epithelial cells of the human thymus express a highly diverse selection of tissue-specific genes colocalized in chromosomal clusters. J Exp Med 2004;199:155–166. [PubMed: 14734521]
52. Bonilla IE, Tanabe K, Strittmatter SM. Small proline-rich repeat protein 1A is expressed by axotomized neurons and promotes axonal outgrowth. J Neurosci 2002;22:1303–1315. [PubMed: 11850458]
53. Fischer D, Petkova V, Thanos S, Benowitz LI. Switching mature retinal ganglion cells to a robust growth state in vivo: gene expression and synergy with RhoA inactivation. J Neurosci 2004;24:8726–8740. [PubMed: 15470139]
54. Morris JS, Stein T, Pringle MA, Davies CR, Weber-Hall S, Ferrier RK, et al. Involvement of axonal guidance proteins and their signaling partners in the developing mouse mammary gland. J Cell Physiol 2006;206:16–24. [PubMed: 15920758]
55. Robertson FG, Harris J, Naylor MJ, Oakes SR, Kindblom J, Dillner K, et al. Prostate development and carcinogenesis in prolactin receptor knockout mice. Endocrinology 2003;144:3196–3205. [PubMed: 12810576]
56. Moggs JG, Tinwell H, Spurway T, Chang HS, Pate I, Lim FL, et al. Phenotypic anchoring of gene expression changes during estrogen-induced uterine growth. Environ Health Perspect 2004;112:1589–1606. [PubMed: 15598610]
57. Park YK, Franklin JL, Settle SH, Levy SE, Chung E, Jeyakumar LH, et al. Gene expression profile analysis of mouse colon embryonic development. Genesis 2005;41:1–12. [PubMed: 15645444]

NIH-PA Author Manuscript

NIH-PA Author Manuscript

NIH-PA Author Manuscript

58. Daimon Y, Yamanishi K, Murakami Y, Kirishima T, Ito Y, Minami M, et al. Novel single nucleotide polymorphisms of the cytokeratin 19 pseudogene are associated with primary biliary cirrhosis. Hepatol Res 2003;25:281–286. [PubMed: 12697249]

59. Lee G. Tau and src family tyrosine kinases. Biochim Biophys Acta 2005;1739:323–330. [PubMed: 15615649]

Abbreviations in this paper

BEC
Biliary Epithelial Cell

C-SFM
Complete Serum-free Medium

EDC
Epidermal Differential Complex

EMT
Epithelial-mesenchymal Transition

HMGB1
High Mobility Group Box 1

PBC
Primary Biliary Cirrhosis

SPRR protein
Small Proline-rich protein

ROS
reactive oxygen species

STAT3
Signal Transducer and Activator of Transcription 3

NIH-PA Author Manuscript
NIH-PA Author Manuscript
NIH-PA Author Manuscript

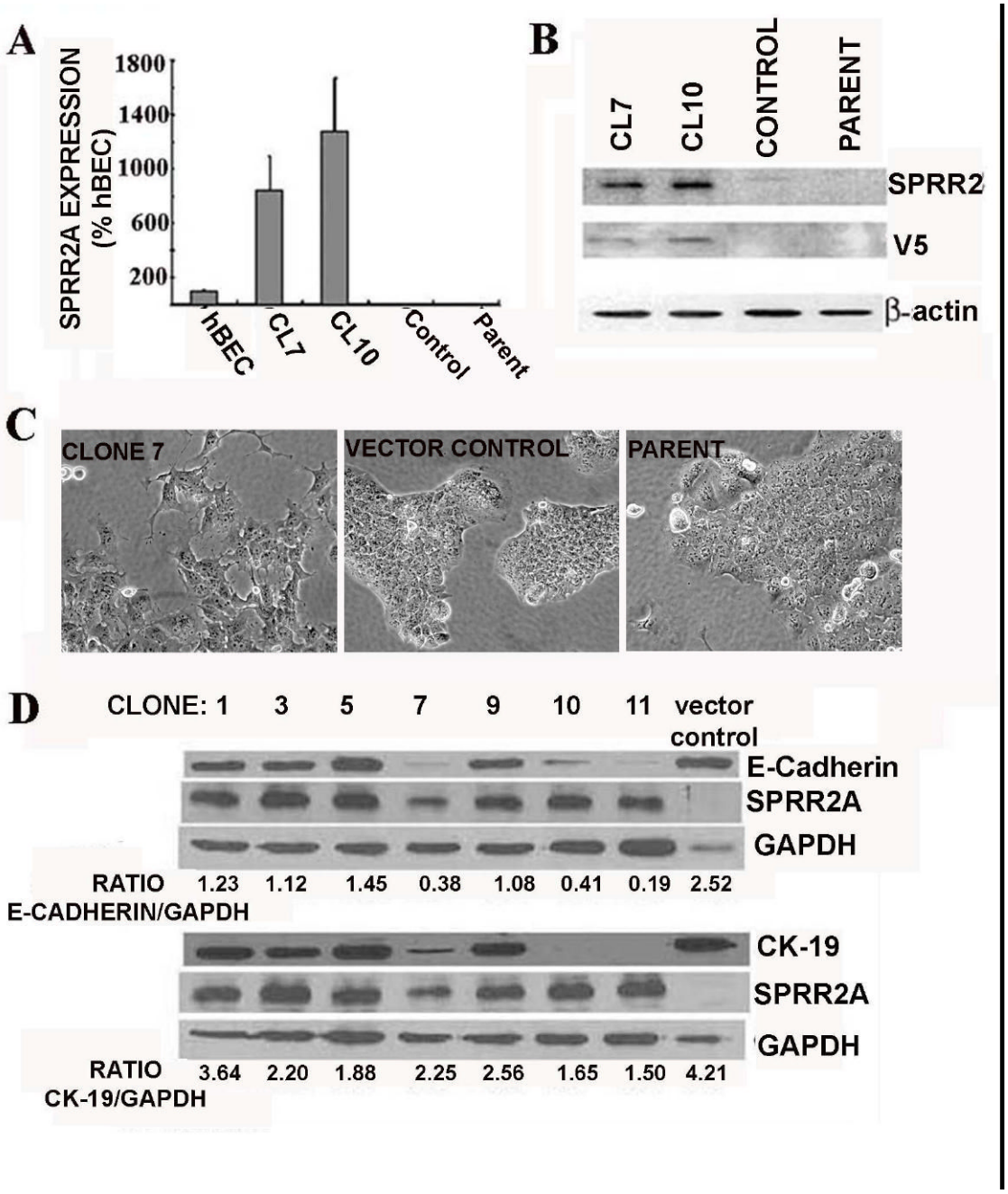

Figure 1.

Stable expression of SPRR2A in SG231 cells results in changes of cell shape and emergence of mesenchymal characteristics. **A)** SPRR2A mRNA by real-time PCR and **B)** protein (V5 tag) expression by Western blot in stable transfectants, clone 7 (CL7) and clone 10 (CL10), was quantified and compared to primary human BEC (hBEC) cultures; the SG231 parental cell line, which showed very little SPRR2A mRNA expression; and SG231 stably transfected with a control vector (Control). **C)** Phase-contrast photomicrographs (72 hour) of a SPRR2A transfectant (clone 7; left panel) was compared to a control transfectant (Control; middle panel), and SG231 (Parent; right panel) cells. Note that non-coordinate SPRR2A expression in clone 7 resulted in decreased intercellular junctions, larger cell size, and a dendritic or spindle-shaped

morphology. Multi-nucleation was also occasionally seen. **D)** E-cadherin, CK-19, SPRR2 and V5 (tagged to SPRR2), protein expression was analyzed by Western blot and compared to GAPDH protein levels. All SPRR2A stable transfectants have reduced CK-19 and E-cadherin expression relative to the vector control.

NIH-PA Author Manuscript
NIH-PA Author Manuscript
NIH-PA Author Manuscript

NIH-PA Author Manuscript
NIH-PA Author Manuscript
NIH-PA Author Manuscript

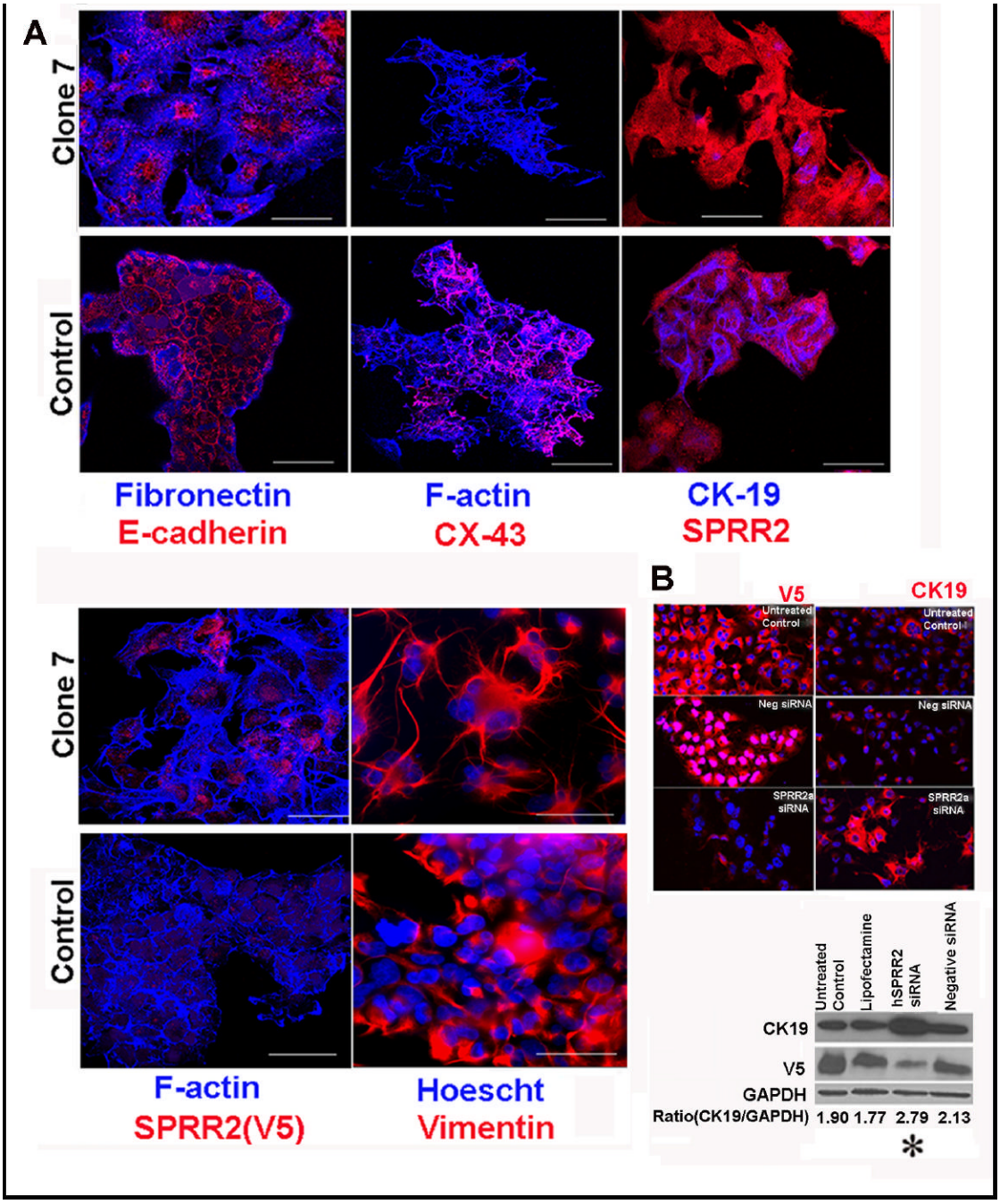

Figure 2.

Phenotypic characterization of SG231 cells after SPRR2A transfection. **A)** In the control transfectant (Control), E-cadherin and connexin-43 localized to the cell surface at intercellular borders; cytokeratin-19 localized to the cytoplasm (58); fibronectin localized to the edge of cell colonies; and F-actin fibers localized just beneath and parallel to the plasma membrane, typical of epithelial cells. In contrast, the SPRR2A transfectant (Clone 7) showed loss of membranous staining for E-cadherin and connexin-43; and significantly decreased cytoplasmic staining for CK19; F-actin reorganized into long cytoplasmic stress fibers; fibronectin localized to cytoskeletal fibers; and vimentin formed distinct cytoplasmic bundles. These characteristics are more typical of mesenchymal cells. **B)** SPRR2A-induced decreased CK-19 expression is

reversed with SPRR2A siRNA treatment. Relative expression of CK-19 in clone 7 was measured by immunofluorescence staining (red) and western blotting when cells were either untreated (untreated control), or treated with lipofectamine, negative siRNA, or SPRR2A siRNA. Immunofluorescence staining (red) and western blotting for the V5 tag verified siRNA knock-down of SPRR2A expression.

NIH-PA Author Manuscript
NIH-PA Author Manuscript
NIH-PA Author Manuscript

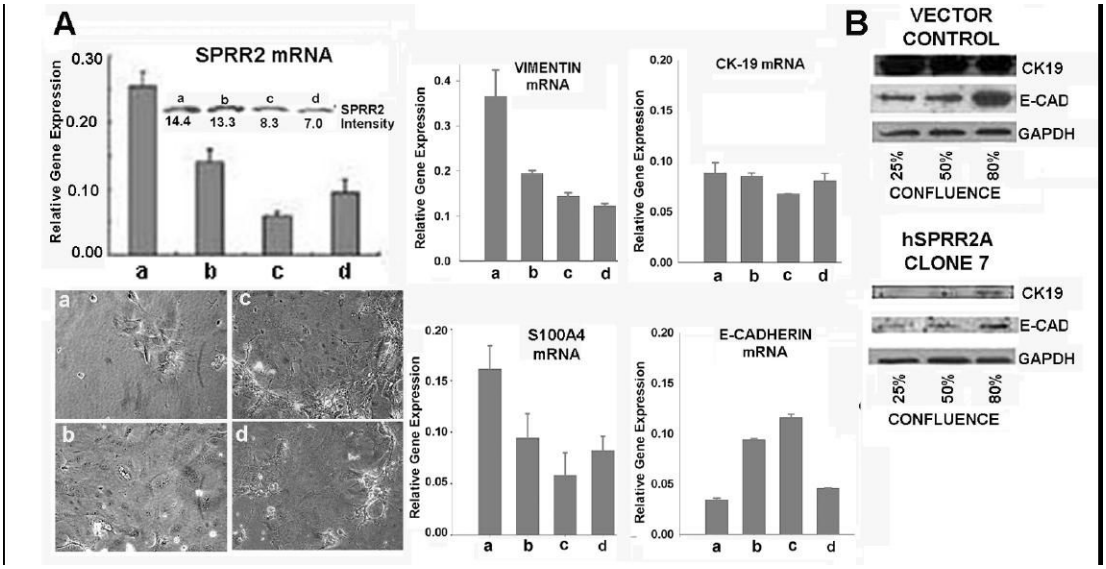

Figure 3.

A) SPRR2A, vimentin, S1004A and E-cadherin mRNA expression is affected by cell confluency in primary mouse BEC cultures. BEC were inoculated at increasing cell numbers: 25 (a), 50 (b), 100 (c), 200 (d) X 10^3 cells/ well and pictures were taken at 48 hours, immediately before RNA and protein were extracted for quantification. Intensity of SPRR2 protein bands were quantified by densitometry. **B)** Expression of the epithelial markers (cytokeratin-19 and E-cadherin) in Clone 7 is also dependent on the level of confluence in both transfectants and the vector control. For each confluence level, equal numbers of cells were seeded in tissue culture wells and collected at 24 hours for Western blot analysis. These observations are consistent with the tendency of clone 7 to maintain a front row phenotype and reluctance of clone 7 to form typical cobblestone sheet, in vitro.

NIH-PA Author Manuscript NIH-PA Author Manuscript NIH-PA Author Manuscript

NIH-PA Author Manuscript

NIH-PA Author Manuscript

NIH-PA Author Manuscript

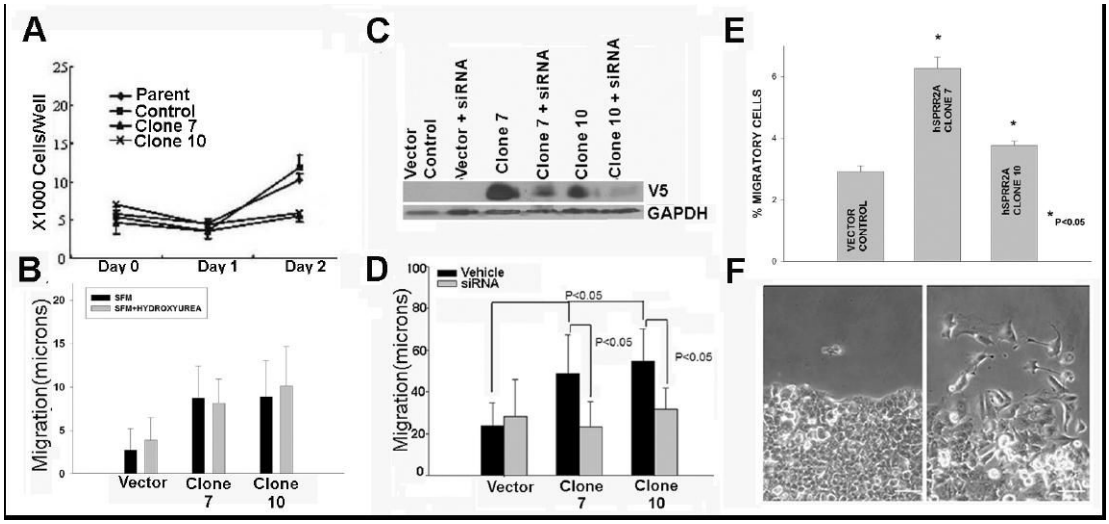

Figure 4.

SPRR2A transfectants (clone 7 and 10) proliferate less, but show better migration from the acellular front of a wound than vector control transfectants. **A)** Cell proliferation was measured 24 hours after seeding in serum supplemented media (SSM) (Day 0). Media was then changed to serum free media (SFM) and cell counts were obtained by trypan blue staining at 24 (Day 1) and 48 (Day 2) hours. No measurable proliferation is seen in the cells during the first 24 hours incubation in SFM. **B)** 5 nmol/L hydroxyurea (Sigma, St. Louis, MO) was used to prevent cell proliferation and migration distances measured 24 hours after wounding of monolayers in SFM ± hydroxyurea. No significant difference in migration distances is seen in the presence or absence of hydroxyurea. Therefore, enhanced migration exhibited by SPRR2A clones can not be attributed to proliferation. **C-D)** Cells in SSM with lipofectamine (vehicle) or lipofectamine + SPRR2A siRNA were seeded at sufficient numbers to generate confluent monolayers and incubated for 72 hours. The media was changed to SFM, monolayers wounded, and migration distances measured after 24 hours. SPRR2 induced migration was reversed with siRNA knockdown of SPRR2A, which was confirmed by Western blot . Cell counts at the end of the experiment verified that the enhanced migration was not due to increased proliferation. **E)** The number of cells able to traverse the membrane of a transwell (8μm pore) confirms SPRR2 clones have greater migratory ability. Cells were seeded into the upper chamber of a transwell in SSM and given 24 hours to migrate through to the bottom chamber. Percent migration ± SE is shown. **F)** A photomicrograph shows little migratory activity from vector control cells (left panel) while SPRR2A transfectants (right panel) migrate readily from the wound front.

NIH-PA Author Manuscript
NIH-PA Author Manuscript
NIH-PA Author Manuscript

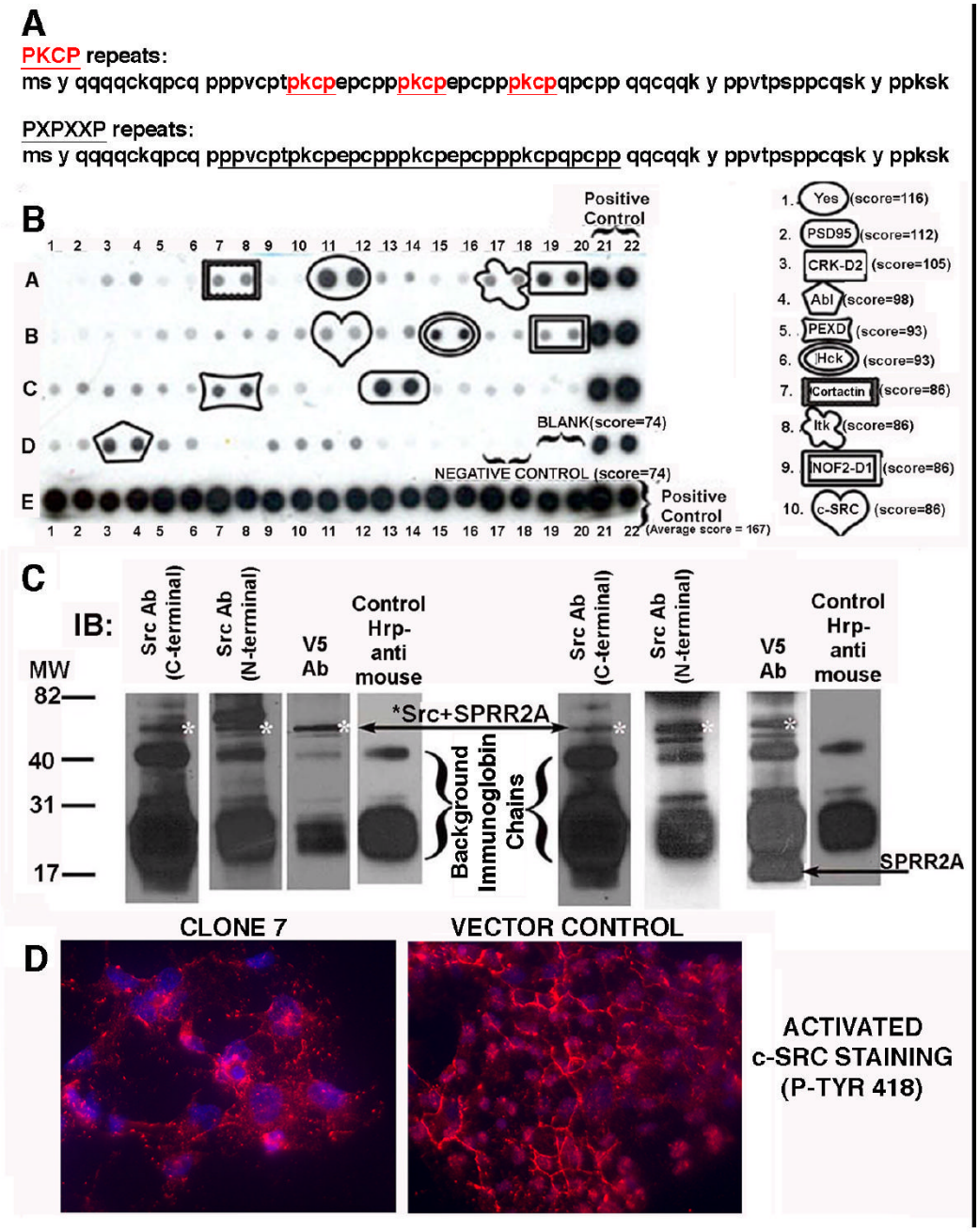

Figure 5.

SPRR2A contains ligands that bind to SH3 domain-containing proteins. **A)** Mapping of the SH3 ligand motifs in SPRR2A. The seven-residue core SH3 ligand consensus sequence, pXPpXP (where small p = proline-preferred and X tend to be aliphatic), occurs several times in the underlined region of SPRR2A. The two prolines are crucial for high affinity binding. Additionally, Tau, a neural protein is known to activate Src with an interaction PXXP motif (59). A PKCP motif is also repeated in SPRR2A. **B)** We transfected BL21 *E. coli* with a hSPRR2A-his-V5 tagged plasmid and induced protein expression with ITPG. The SPRR2A protein was purified from the bacterial lysate using a His-column. The effluent was applied to an SH3 binding domain array (Promega BioSciences, San Luis Obispo, CA) and visualized

NIH-PA Author Manuscript

NIH-PA Author Manuscript

NIH-PA Author Manuscript

using a mouse anti-V5 antibody. The top 10 significant interactions of SPRR2A protein to the SH3 binding Domain include: Yes, CRK-D2, Abl, Cortactin (important for actin assembly and intimately associated with SFK signaling), Itk, and c-Src. The array also shows SPRR binding to PEXD and Hck, but these are not expressed by the cell line (data not shown). Expression of PSD95 and NOF2-D1 in vector control or clone 7 is as yet undetermined. Relative scores were determined by densitometry using Image J software. **C)** Immunoprecipitation of protein extracted from clone 7 with mouse monoclonal anti-c-Src or anti-V5 specific antibodies shows the interaction of Src tyrosine kinase (60kDa) with SPRR2A-V5 protein (14kDa). Left immunoblot (IB): Immunoprecipitation performed with c-Src antibody (N-terminal) and the western blot developed with Src and V5 antibodies. One band is clearly identified where both proteins co-localize (*). Right IB: Immunoprecipitation performed with V5 antibody and the blot developed with Src and V5 antibodies. The same band is identified where Src and SPRR2A are associated (*). In addition, free SPRR2A protein was also immunoprecipitated. Background mouse immunoglobulins used to perform the immunoprecipitation are visualized by developing the blot with secondary antibody only (HRP-anti mouse) so these bands can be excluded from the analysis. **D)** Localization of activated Src (P-Tyr 418) by immunofluorescence using Cy3 secondary antibody (red) and Hoechst dye nuclear staining (blue) yields a linear-punctuate cytoplasmic staining in clone 7 with only occasional localization at cell-cell junctions. In contrast, vector controls show activated Src along the cell membrane resulting in a linear staining pattern. (Magnification 400X).

NIH-PA Author Manuscript

NIH-PA Author Manuscript

NIH-PA Author Manuscript

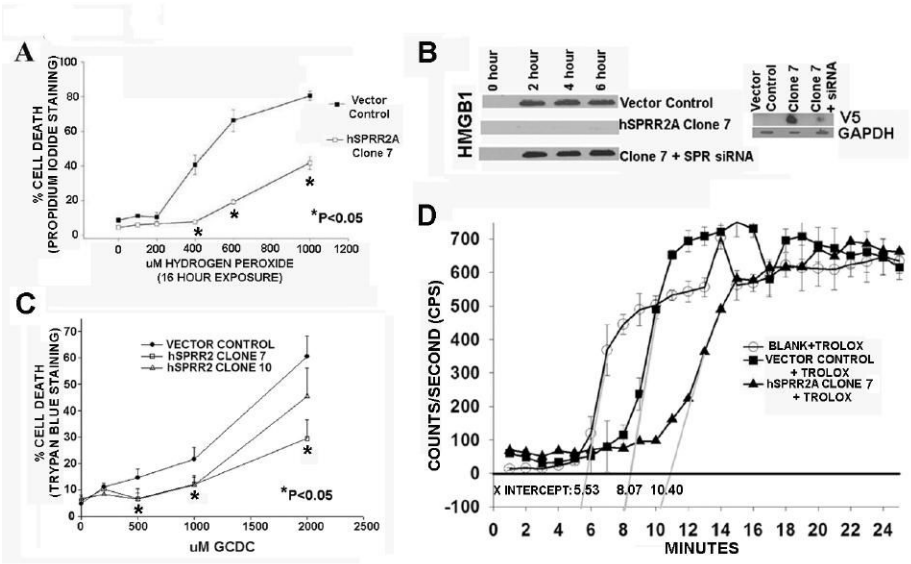

Figure 6.

Non-coordinate SPRR2A expression increases resistance to injury. **A)** Cell death was measured by flow cytometry for propidium iodide staining of non-viable cells and shows that the SPRR2A transfectants are more resistant to H_2O_2 exposure than the vector control. **B)** Knockdown of SPRR2A by SPRR2A specific siRNA increased the amount of HMGB1 released into the culture supernatant after exposure to 1500μM H_2O_2. HMGB1 released into the supernatant was used to measure necrotic cell death by Western blot. Cells were treated with lipofectamine only or SPRR2A siRNA for 72 hours and then exposed to 1500μM H_2O_2 in serum free media. Prior to H_2O_2 treatment, knockdown of SPRR2A expression was verified by Western blot for V5. **C)** Cell death was also measured by trypan blue staining following exposure to glycochenodeoxycholate (GCDC) for 4 hours. SPRR2A clones were more resistant to GCDC than the vector control. **D)** The anti-oxidant potential of the SPRR2A clones is measured in a TRAP assay. A representative TRAP assay shows that 5μg cytosol from SPRR2A clone 7 has a greater anti-oxidant capacity than the vector control. Clone 7 cytosol produces a significant extension of the Trolox® induction time when compared to the vector control. Each TRAP graph represents an average of n=4 samples and was repeated at least twice.

NIH-PA Author Manuscript
NIH-PA Author Manuscript
NIH-PA Author Manuscript

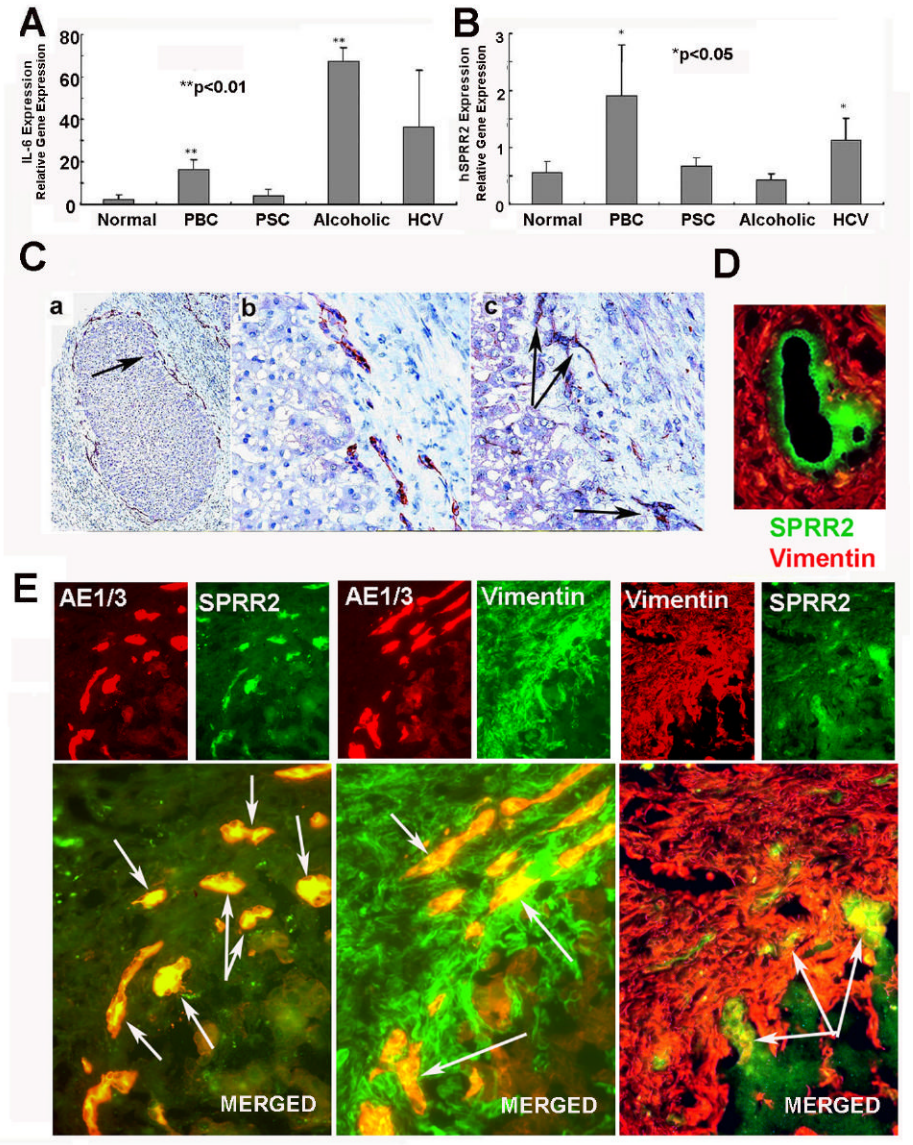

Figure 7.

A) Expression of IL-6 and **B)** SPRR2A mRNA by quantitative real time PCR in human liver tissue removed at the time of transplantation. Consistent with a role in response to stress, SPRR2A showed some upregulation in almost all liver diseases, but the upregulation was most significant in PBC ($n \geq 3$ for each disease). (PBC=primary biliary cirrhosis; PSC=primary sclerosing cholangitis; HCV=hepatitis C viral infection) **C)** Immunoperoxidase staining showed that SPRR2 expression was limited to BEC. AE1/3 $^{+}$ atypical cholangioles (a) and (b) at the interface zone of a human liver with PBC also showed Sprr2 protein expression (c). **D)** Liver with PBC showed positive staining for Sprr2 in columnar BEC lining a septal bile duct, but these same ducts were negative for vimentin co-expression. **E)** In contrast, double immunofluorescence studies on the same liver and same tissue section showed that some of the atypical cholangioles co-expressed biliary cytokeratin, vimentin, and SPRR2. Serial sections of the same atypical ductular reactions were stained for AE1/3 and SPRR2 (left frame), AE1/3 and vimentin (middle frame), and vimentin and SPRR2 (right frame). Note that some

of the atypical cholangioles express SPRR2, AE1/3 cytokeratin, and vimentin similar to the SPRR2A transfectants and low confluency mouse BEC. Atypical ductular reactions showing EMT were much less common in PSC and chronic hepatitis (data not shown).

NIH-PA Author Manuscript
NIH-PA Author Manuscript
NIH-PA Author Manuscript

NIH-PA Author Manuscript
NIH-PA Author Manuscript
NIH-PA Author Manuscript

TABLE 1

cDNA microarray studies showing SPRR genes to be among the most highly upregulated genes under the non-neoplastic contexts listed. The studies are grouped together according to organ.

Study	Context (organ/tissue)	SPRR	Findings (species)
Hooper (35)	Infection and adaptation (intestinal epithelium)	SPRR2A	>200-fold increase in ileal epithelium after introduction of *Bacteroides thetaiotaomicron* , a commensal bacteria in the mouse (mice)
Knight (36)	Parasite infection, inflammation/stress, and remodeling/repair (intestine)	SPRR2A	37-fold increase in jejunal epithelial cells after infection with *Trichinella spiralis* (mice)
Abgueguen (37)	Oxidative stress in (duodenal epithelium)	SPRR2A	Induced expression in Hfe-/- mice and after iron treatment of wild type mice (mice)
Mueller (38)	Infection, inflammation/stress, and remodeling in (stomach epithelium)	SPRR2A	Highest up-regulated gene after Helicobacter infection of stomach epithelium (mice)
Stern (39)	Regeneration/remodeling and adaptation in (small intestine)	SPRR2	4-fold induction after massive small bowel resection (mice)
Sun (40)	Infection/inflammation/stress in gastrin-deficient mice (stomach)	SPRR2A	Increased after introduction of bacteria into stomach. (mice)
Tan (41)	Estrogen-responsive genes, remodeling (uterus)	SPRR2A	10-fold (highest) induced expression of SPRR2A in uterine epithelium during estrogen phase (mice).
Hong (42)	Implantation site, remodeling, and repair (uterus)	SPRR2A	~10-fold increase at implantation site (mice)
Nozaki (5)	Biomechanical stress, inflammation, morphogenesis, and repair in (liver/biliary epithelium)	SPRR2A	>15-30-fold increase after bile duct ligation and in cell cultures after IL-6-induction (mice and humans)
Zimmerman n (43)	Allergic inflammation/stress, repair (lung)	SPRR2A, SPRR2B	~10-fold induction in lung and intestinal epithelium after antigen-induced allergic inflammation (mice)
Vos (44)	Infection/stress (lungs)	SPRR1B, 2A	Highly upregulated after exposure of cultured human bronchial epithelial cells to cytokines and bacteria (human)
Domachows ke (45)	Infection, inflammation/stress (lungs)	SPRR1A	Differentially regulated according to pathogenic (upregulated) or non-pathogenic viral lung infection (down-regulated) (mice).
Sandler (46)	Inflammation/stress, and remodeling (lungs)	SPRR	Upregulated in lungs of mice challenged with parasite eggs; especially high levels detected in TH-2-prone mice (mice)
Yoneda (47)	Stress (smoke or H_2O_2 exposure) of bronchial epithelium (lungs)	SPRR1A	Upregulated 10 hrs after smoke exposure along with other genes in metabolism of oxidants or involved in tissue remodeling (human).
Kawasaki (48)	Inflammation/stress, injury, and repair (cornea)	SPRR2A	Comparison of normal corneal epithelium to Sjogren's syndrome (humans)
Young (49)	Atherosclerotic plaques, inflammation/ stress (arterial intima)	SPRR3	20-300 X levels seen in skin (mice and human)
Pradervand (50)	Biomechanical/ischemic stress and remodeling (heart)	SPRR1A, SPRR2A	2-35-fold induction 4 days after pressure over load or after one week in myocytes near infarcts; myocytes with transduced expression showed resistance to ischemic injury (mice)
Gotter (51)	Cultured (thymic epithelium)	SPRR1B	SPRR upregulated in cultured thymic epithelium; likely related to squamous differentiation (human)
Bonilla (52)	Nerve injury, axonal outgrowth, remodeling, repair (peripheral nerves)	SPRR1A	> 60-fold induction in injured peripheral neurons; associated with axonal outgrowth (mice)
Fischer (53)	Injury, growth, and remodeling in (central neurons)	SPRR1A	One of highest (> 4-fold) increase in retinal ganglion cells after injury (rat)
Morris (54)	Development and morphogenesis (breast)	SPRR1A, 2A, 2B	6-12 fold increase as breast bud penetrates mesenchyme (mice)
Robertson (55)	Development and morphogenesis (prostate)	SPRR2A	Upregulated during prostate development and carcinogenesis in prolactin receptor knockout mice (mice)
Moggs (56)	Hormone-responsive remodeling (uterus)	SPRR1,2	5-60-fold estrogen-induced upregulation during uterine epithelial remodeling (mice)
Park (57)	Development and morphogenesis (colon)	SPRR2A	Four-fold or greater increase of between E13.5 and E18.5 development, associated with "differentiation".

NIH-PA Author Manuscript

NIH-PA Author Manuscript

NIH-PA Author Manuscript

TABLE 2

(m = mouse; h = human)

Sequence	Forward Primer (5’-3’)	Reverse Primer (5’-3’)
mSPRR2A	CCTTGTCCTCCCCAAGCG	AGGGCATGTTGACTGCCAT
mCK-19	ACCCTCCCGAGATTACAACC	CAAGGCGTGTTCTGTCTCAA
mVIMENTIN	AAGGAAGAGATGGCTCGTCA	TTGAGTGGGTGTCAACCAGA
mE-CADHERIN	GTCAACACCTACAACGCTGCC	GTTGTGCTCAAGCCTTCAC
mGAPDH	TGGCAAAGTGGAGATTGTTGCC	AAGATGGTGATGGGCTTCCCG
mS100A4	TTGTGTCCACCTTCCACAAA	GCTGTCCAAGTTGCTCATCA
hSPRR2A	AGTGCCAGCAGAAATATCCTCC	TGCTCTTGGGTGGATACTTTGA
hβ-ACTIN	AGGCATCCTCACCCTGAAGTA	CACACGCAGCTCATTGTAGA

NIH-PA Author Manuscript

NIH-PA Author Manuscript

NIH-PA Author Manuscript

TABLE 3

Primary Antibodies	Conjugate	Source
mouse anti-V5	unconjugated	Invitrogen, Carlsbad, CA
mouse anti-Cytokeratin 19	unconjugated	BioGenex, San Ramon, CA
mouse-anti-E-Cadherin	unconjugated	BD Biosciences, San Diego, CA
mouse-anti-β-actin(cone AC-15)	unconjugated	Sigma-Aldrich, Saint Louis, MO
mouse-anti-GAPDH	unconjugated	Ambion, Austin, TX
mouse-anti-C-Src (B-12)	unconjugated	Santa Cruz Biotechnology, Inc., Santa Cruz, CA
mouse-anti-C-Src (H-12)	unconjugated	Santa Cruz Biotechnology, Inc., Santa Cruz, CA
rabbit anti-HMGB1	unconjugated	PharMingen, San Diego, CA
Rabbit anti-SPRR2A	unconjugated	Apotech Corporation, Geneva Switzerland
mouse anti-AE1/3	unconjugated	Dako, Carpenteria, CA
rabbit anti-fibronectin	unconjugated	Dako, Carpenteria, CA
mouse anti-vimentin	unconjugated	BioGenex, San Ramon, CA
rabbit anti-phospho-Src (pTyr 418)	unconjugated	Sigma-Aldrich, Saint Louis, MO
phalloidin	Cy5	Invitrogen, Carlsbad, CA
Secondary Antibodies	**Conjugate**	**Source**
Donkey anti-rabbit IgG	HRP	Amersham, Buckinghamshire, UK
Sheep anti-mouse IgG	HRP	Amersham, Buckinghamshire, UK
goat anti-mouse IgG	Cy3 or Cy5 or FITC	Jackson ImmunoResearch Laboratories, West Grove, PA
goat anti-rabbit IgG	Cy3 or Cy5 or FITC	Jackson ImmunoResearch Laboratories, West Grove, PA